Section 4

Parameterization of important atmospheric and surface processes, effects of different parameterizations

Modelling of active layer dynamics and talik formation

M.M. Arzhanov
A.M. Obukhov Institute of Atmospheric Physics RAS, 3 Pyzhevsky, 119017 Moscow, Russia
e-mail: arzhanov@ifaran.ru

Active layer dynamics is assessed using the numerical model for thermal and hydrological processes in soil (Arzhanov et al., 2008; Mokhov et al., 2009) for geocryologival stations Marre-Sale (69ºN, 66ºE) and Yakutsk (129ºN, 62ºE). Atmospheric forcing needed by the model is taken either from the ERA-40 reanalysis data (Uppala et al., 2005) or from output from simulations with a coupled atmosphere-ocean general circulation model ECHAM5/MPI-OM . Figure 1 shows the comparison of simulated active layer thickness using ERA-40 reanalysis and observed active layer thickness for the Marre-Sale (Izrael et al., 2002; Pavlov and Moskalenko, 2002) and Yakutsk (Konstantinov et al., 2006) stations for the 1980s and 1990s.

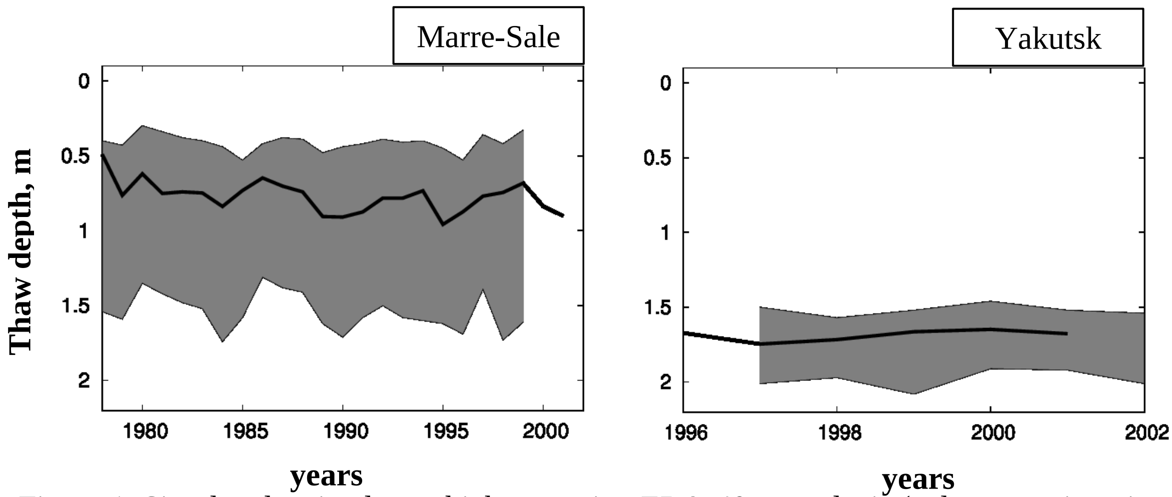

Figure 1. Simulated active layer thickness using ERA-40 reanalysis (values are given in black) and observations (values are given in gray) for the Marre-Sale and Yakutsk stations.

The simulated and observed active layer thickness are in reasonably good agreement for the both stations. For the Marre-Sale station, a general tendency for an increase the active layer thickness was observed in 1978-1995 (Pavlov and Moskalenko, 2002). The simulated active layer trend at the Marre-Sale station is about 0.007 m per year during the 1978-1995 period. Observed trends are about 0.005-0.011 m per year for this period (Izrael et al., 2001). The period from 1996 to 1999 was characterized by colder mean annual and summer temperatures. As a result, tendency for an increase in the thaw depth becomes less pronounced (Fig. 1).
To assess active layer dynamic for the Marre-Sale and Yakutsk stations during the 21st century the permafrost model was forced by the ECHAM5/MPI-OM atmospheric characteristics under SRES A1B and A2 scenarios. Summer air temperature increased by 4.8ºC at A1B scenario and 5.9ºC at A2 scenario for the Marre-Sale and increased by 4.0ºC and 5.3ºC, respectively, for the Yakutsk from 2000s to the 2090s (Fig. 2a). Thaw depth increased from the 2000s to the 2050s for the Marre-Sale station and from 2000s to the 2070s for the Yakutsk station (Fig. 2b). Since 2050s, the near-surface frozen ground thawed and talik depth increased for the Marre-Sale. The results also show that changes thawing regimes were different due to the summer air temperature (about 1.8ºC for the 2040-2060) under A1B and A2 scenarios. For the Yakutsk station the first talik formation occurred about 2073-2075 (Fig. 2b) and then talik depth increased since 2080s.

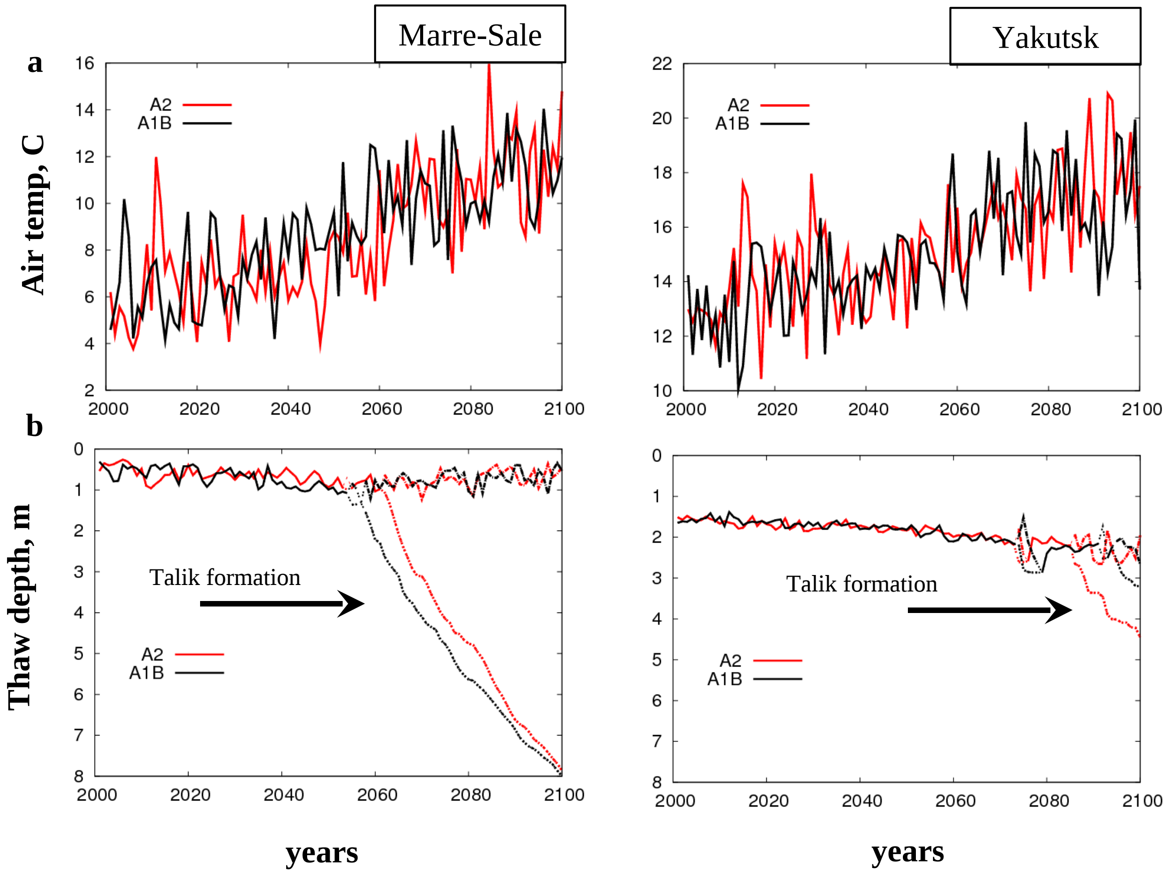

Figure 2. Summer air temperature under SRES A1B, A2 scenarios (a) and simulated thaw depths (b) for the Marre-Sale and Yakutsk stations.

Acknowledgements

The World Climate Research Programme's (WCRP's) Coupled Model Intercomparison Project phase 3 (CMIP3) multi-model dataset;

Russian Foundation for Basic Research, grants no. 07-05-00164, 07-05-00273, 08-05-00458, 08-05-00532, 09-01-00226, 09-05-00564.

References

Arzhanov M.M., Eliseev A.V., Demchenko P.F., Mokhov I.I. and Khon V.Ch. Simulation of thermal and hydrological regimes of Siberian river watersheds under permafrost conditions from reanalysis data // Izvestiya Atmospheric and Oceanic Physics. 2008. V.44. N.1. P.83-89.

Izrael Yu.A., Pavlov A.V., Anokhin Y.A. Evolution of the Cryolithozone Under Present-Day Global Climate Changes // Russian Meteorology and Hydrology. 2002. N.1. P.22-34.

Konstantinov P.Ya., Argunov R.N., Gerasimov E.Y., Ugarov I.S. On the relationship between seasonal thaw depth and interannual variation of mean annual ground temperature // Earth Cryosphere. 2006. Vol.X. N.3. P.15-22.

Mokhov I.I., Eliseev A.V., Arzhanov M.M., Demchenko P.F., Denisov S.N. Climate changes in the northern Eurasia simulated by two models of different complexity // IOP Conference Series: Earth and Environmental Science. Climate Change: Global Risks, Challenges and Decisions. 2009. V.6. P.052021.

Pavlov A.V., Moskalenko N.G. The thermal regime of soils in the north of Western Siberia // Permafrost and periglacial processes. 2002. V.13. P.43-51.

Uppala S.M., Kellberg P.W., Simmons A.J., Andrae U. et al. The ERA-40 re-analysis // Quart. J. R. Meteorol. Soc. 2005. V.131. P.2961-3012.

Improvement of the subgrid vertical mixing parameterization in operational hydrostatic models at Météo-France

Yves Bouteloup, Eric Bazile, François Bouyssel and Pascal Marquet
CNRM/GAME, Météo-France and CNRS
42 av Coriolis, 31057 Toulouse FRANCE
yves.bouteloup@meteo.fr

A global variable mesh model (ARPEGE), an hydrostatic limited area model (ALADIN) with a 9.5km resolution over several regions of the world and a non-hydrostatic 2.5km resolution model (AROME) over France are used operationally at Météo-France for weather forecasting. Important modifications of the subgrid vertical mixing parameterization used in the hydrostatic models became operationnal in February 2009. The Louis scheme (Louis, 1979) associated to a pseudo-shallow convection parameterization (Geleyn, 1987) has been replaced by a prognostic Turbulent Kinetic Energy scheme (TKE) associated to a mass flux shallow convection scheme. This development is characterised by a broad convergence between the parameterizations used in hydrostatic models with those of the operationnal non-hydrostatic model AROME.

The prognostic TKE scheme (Cuxart et al, 2000) is used with the tuning coefficients of AROME. The mixing length is computed using the formulation of Bougeault and Lacarrère (1989) (BL89) but with a modified combination between L_{up} and l_{down}. To improve the representation of stratocumulus, the scheme uses a top-Planetary Boundary Layer (PBL) entrainment parameterization following the ideas of Grenier and Bretherton (2001), with a modified integral formulation.

The shallow convection mass flux scheme is described in Bechtold et al. (2001). To avoid a double counting, the fluxes coming from the deep convection scheme are set to zero when the deep cloud has a height less than 3000m. Finally the condensation coming from the shallow convection scheme is an input of the micro-physics scheme, which means that the shallow convection scheme may indirectly generate precipitations. These two points have a very interesting impact on the quality of the precipitation forecast, mainly in summer (Figure 1).

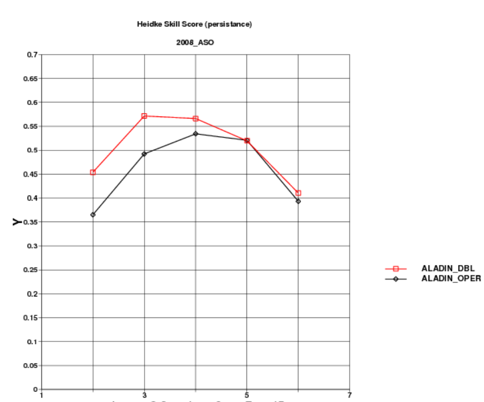

Figure 1 : Heidke Skill Score of the operational (red) and the old-operational (black) ALADIN France model during August, September and October 2008. All the precipitation classes are improved.

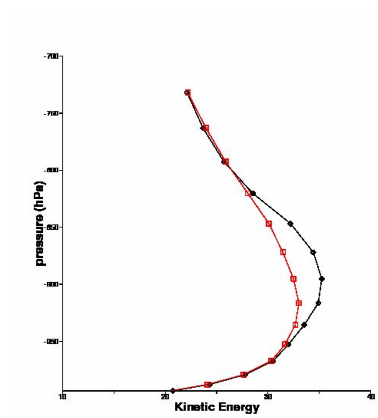

Figure 2 : Zonal mean over tropical area of the Kinetic energy (J/kg) with (red) and without (black) the connection of the turbulence scheme and mass flux shallow convection scheme. The benefical effect in the cloud layer is shown.

To solve a problem of too strong wind in the tropical PBL, it was decided to amend both the mixing length and the TKE, following the approach of Lock and Mailhot (2006). The main idea of the connection between the shallow convection scheme and the turbulence scheme is to suppose that in a PBL, where occurs shallow convection, the turbulent mixing is enhanced by the presence of clouds. First, a thermal production term of TKE coming from the shallow convection scheme is computed. Secondly, a local modification of the BL89 mixing length is used. The BL89 mixing length is computed using the dry buoyancy and doesn't take into account the phase changes of water. In a cloud layer the result is an underestimation of the mixing length. The new approach consists of getting the thickness of the cloud from the shallow convection parameterization. When a shallow convection cloud is present L_{up} (respectively L_{down}) is now taken at least equal to the distance between the current level and the top (respectively the bottom) of the cloud.

By construction this modification has no impact when shallow convection is not active. The impact in the case of PBL with shallow convection cloud, mainly in the tropical area, is very important and leads to a large improvement of the global model ARPEGE (figure 2)

Changes outlined in this paper have a very important impact on the behaviour of the Météo-France hydrostatic models. The main result is a better thermodynamical representation of the PBL, with a large improvement of the low-cloud forecast (figure 3). The connection between the turbulence scheme and the shallow convection scheme is necessary, in ARPEGE, to avoid too strong wind in the tropical PBL. Limited area model ALADIN takes benefit of these modifications in the simulation of low-cloud and fog, but also in the quality of the precipitation fields..

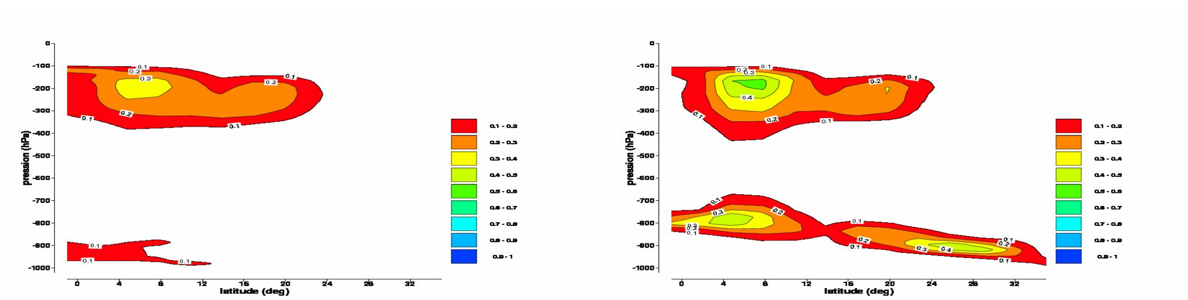

Figure 3 : Cloud cover of the old_operational ARPEGE model (left) for June 2007 along the GEWEX Pacific cross-section which starts from the Equator at 190° East to end by 35° North and 235° East close to Californian coast. Eastern stratocumulus are absent. Right : Same but with the operational model. Eastern Pacific statocumulus are now simulated.

1:Bechtold, P., Bazile, E., Guichard, F., Mascart, P. and Richard, E., 2001 : A mass-flux convection scheme for regional and global models. *Quart. J. R. Met. Soc.*, **127**, p.869-886.
2. Bougeault, Ph., and Lacarrère, P., 1989 : Parameterization of orography-induced in meso-beta-scale model. *Mon. Wea. Rev.*, **117**, p.1872-1891.
3. Cuxart, J., Bougeault, Ph. And Redelsperger, J-L., 2000 : A turbulence scheme allowing for mesoscale and large-eddy simulations. *Quart. J. R. Met. Soc.*, **126**, p.1-30.
4. Geleyn, J.F., 1987 : Use of a modified Richardson number for parameterizing the effect of shallow convection. Short-and Medium-Range Numerical Weather Prediction (also WMO/IUGG NWP Symposium special issue), Tokyo, 4-8 August 1986). Special Volume of *J. Meteor. Soc. Japa*n, T. Matsumo ed., p.141-149.
5. Grenier, H., and Bretherton, C. S., 2001 : A moist PBL parameterization for large scale models and its application ti subtropical cloud-topped marine boundary layers. *Mon. Wea. Rev.*, **129**, p.357-377.
6. Lock, A. and Mailhot, J. 2006 : Combining non-local scalings with a tke closure for mixing in boundary-layer clouds. *Bound.-Layer Meteor.*, **121**, p 313-338.
7. Louis, J.F., 1979 : A parametric model of vertical eddy fluxes in the atmosphere. *Bound. Layer Meteor.*, **17**, p.187-202.

Upgrade of the Radiation Process in the JMA Mesoscale Model

Ryoji Nagasawa
Numerical Prediction Division, Japan Meteorological Agency
1-3-4 Otemachi, Chiyoda-ku, Tokyo 100-8122, Japan
E-mail: r-nagasawa@naps.kishou.go.jp

In response to several issues regarding the radiation process, the three modifications outlined here were found effective for forecast improvement and were implemented into the JMA operational non-hydrostatic mesoscale model (MSM) with a horizontal resolution of 5 km, which has been in operation since March 2006.

Ⅰ. Mitigation of the dependence of longwave radiation calculation on the vertical resolution

In the longwave radiation calculation of the MSM, the effective cloud fraction (i.e., the product of cloud emissivity and the cloud fraction) has conventionally been used. However, Räisänen (1998) pointed out that this value depended on the vertical resolution. Accordingly, the dependence of longwave radiation calculation and the heating rate on the vertical resolution was mitigated by implementing the method of Räisänen (1998) in which longwave radiation is estimated from cloud emissivity and the cloud fraction recurrently. The panel on the left of Fig. 1 shows the difference in the upward longwave radiation flux at TOA (OLR) between 50 and 75 vertical layers MSM calculated using the former method. The cold colors indicate that OLR in the latter is relatively larger than that in the former. On the other hand, the panel on the right of Fig. 1 indicates that OLR has little dependence on the vertical resolution in the method of Räisänen (1998).

Ⅱ. Use of the monthly climatology for aerosol optical depth

The optical parameters (optical depth, single scattering albedo and the asymmetry factor) of various kinds of aerosol were previously parameterized in only two types – continent and marine (see the panel on the left of Fig. 2). Accordingly, more detailed monthly climatology for aerosol optical depth (vertically integrated) retrieved through satellite observation (January 2000 – December 2005) was introduced into the radiation calculation. In the center panel of Fig. 2, aerosol from the Chinese continent is shown arriving over the islands of Japan. This feature of aerosol distribution could not have been considered by the continent- and marine-type aerosol parameterization. However, using the monthly climatology of aerosol optical depth enables consideration of this feature in the radiation calculation of the MSM. Since there were no satellite observations of single scattering albedos and asymmetry factors, these parameters were set into two types (continent and marine) as before. In the panel on the right of Fig. 2, the downward shortwave radiation flux at the surface (clear sky) shows some decrease corresponding to the distribution of the value of the aerosol optical depth.

Ⅲ. Upgrade of the diagnostics method for the effective radius of cloud ice

In the radiation calculation of the MSM, the temperature and effective radius of cloud ice were previously related following Ou and Liou (1995) – a technique that was also used in the former JMA global NWP model (GSM). However, the relationship was optimized for the former GSM, which tended to overestimate the climatology of the effective radius for the MSM in terms of OLR. Accordingly, this relationship was replaced with that of Ou and Liou (1995) modified by McFarquhar et al. (2003).

The three modifications outlined here were included in the operational MSM from December 2008. In the future, upgrades of the diagnostic method for the effective radius of cloud water and modification of treatment regarding the maximum-random overlap in shortwave radiation calculation are planned.

References

McFarquhar, G. M., S. Iacobellis, and R. C. J. Somerville, 2003: SCM Simulations of Tropical Ice Clouds Using Observationally Based Parameterizations of Microphysics. *J. Climate,* **16**, 1643-1664.

Ou, S., and K. N. Liou, 1995: Ice microphysics and climatic temperature feedback. *Atmos. Res.*, **35**, 127-138.

Räisänen, P., 1998: Effective Longwave Cloud Fraction and Maximum-Random Overlap of Clouds. A Problem and a Solution. *Mon. Wea. Rev.,* **126**, 3336-3340.

Saito, K., J. Ishida, K. Aranami, T. Hara, T. Segawa, M. Narita, and Y. Honda, 2007: Nonhydrostatic Atmospheric Models and Operational Development at JMA. *J. Meteor. Soc. Japan*, **85**, 271-304.

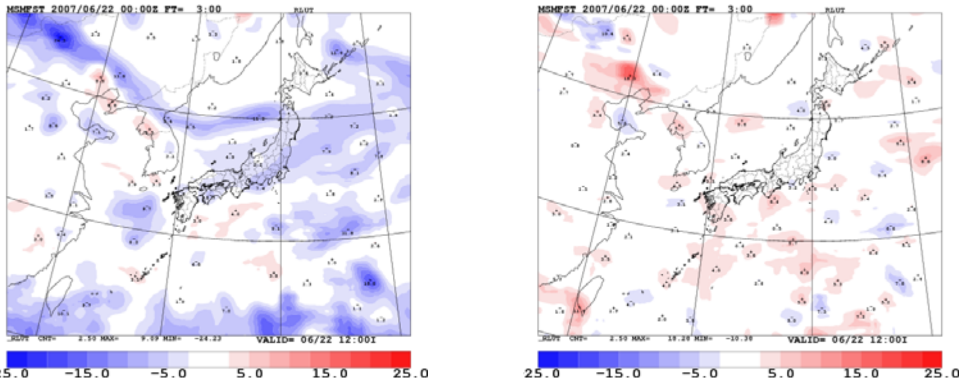

Fig. 1 The difference in the upward longwave radiation flux at TOA (50 vertical layers MSM minus 75 vertical layers MSM) (Wm^{-2}). Left panel: the former method. Right panel: the method of Räisänen (1998). The initial time is 00 UTC on 22 June 2007, and the forecast is for a three-hour period. The model tops are almost the same for 50 and 75 vertical layers.

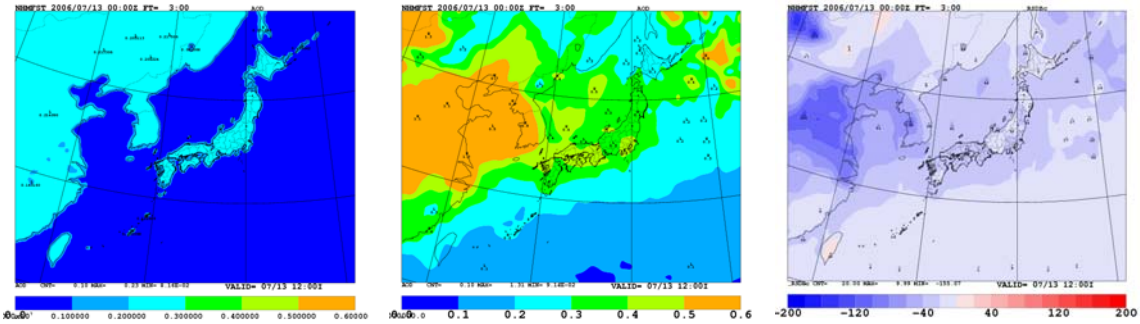

Fig. 2 Left panel: the former climatology for aerosol optical depth (vertical integrated) depended only on land and sea distribution. Center panel: the new monthly climatology for aerosol optical depth (July, vertically integrated). Right panel: the impact of the new climatology for aerosol on the downward shortwave radiation flux at the surface (clear sky) (Wm^{-2}). The initial time is 00 UTC on 13 July 2006, and the forecast is for a three-hour period.

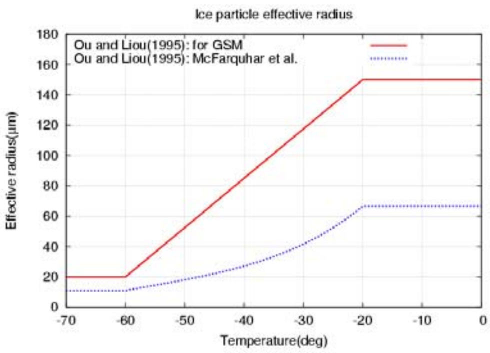

Fig. 3 Relationship between temperature (deg) and the effective radius (μm) of the cloud ice used in the radiation calculation. Red: relationship of Ou and Liou (1995) optimized for the former GSM. Blue: that of Ou and Liou (1995) modified by McFarquhar et al. (2003).

Implementation of Rainwater and Cloud Water Budget in the Cloud Layer into the Cumulus Parameterization Scheme of the JMA Global Model

Masayuki Nakagawa

Numerical Prediction Division, Japan Meteorological Agency

1-3-4 Otemachi, Chiyoda-ku, Tokyo 100-8122, JAPAN

m-nakagawa@met.kishou.go.jp

The cumulus parameterization scheme implemented in the operational Global Spectral Model (GSM) at the Japan Meteorological Agency (JMA) follows the scheme proposed by Arakawa and Schubert (1974) with modifications by Moorthi and Suarez (1992), Randall and Pan (1993) and Pan and Randall (1998). In the scheme of GSM, condensed water in upward cloud mass flux is lifted to the cloud top. Some of this falls as rainwater, and the rest is detrained as cloud water. The ratio of rainwater is assumed to be proportional to the cloud depth. The cloud water is re-distributed to the layer above the freezing level to represent anvil cloud detrained from deep cumulus. This parameterization is quite economical, but may produce errors because of its simplicity.

Miyamoto and Komori (2008) showed that GSM tends to predict drier middle troposphere than radiosonde observation over Japan in the summer season and the NWP models of two other NWP centers (ECMWF and UKMO) in regions where deep convection is active. They concluded that the dry bias is due to deficiencies in the convection process of GSM.

To reduce the dry bias, we are currently developing a modification of the cumulus parameterization scheme. The following three processes are introduced into the modified scheme: (1) generation of rainwater in the updraft (e.g., Cheng and Arakawa 1997); (2) detrainment of rainwater from the updraft (Kuo and Raymond 1980); (3) detrainment of cloud water from the updraft between the cloud base and the cloud top. Cloud water is assumed to detrain at the same rate as rainwater. We also assume that only frozen water contents detrain below the cloud top to represent anvil cloud. The convective downdraft process is also upgraded to allow calculation of the downdraft ensemble corresponding to the updraft ensemble. In addition, the evaporation process of convective rain is revised to the version proposed by Kessler (1969).

In order to evaluate forecast skill, forecast/assimilation experiments using the operational GSM (CNTL) and the modified GSM (TEST) were conducted for August 2008. Figure 1 shows the averages of the mean errors (ME) of specific humidity in 48-hour forecasts against radiosonde observations over the tropics. It can be seen that the dry bias around 700 hPa seen in CNTL is reduced substantially in TEST. This reduction is caused by the

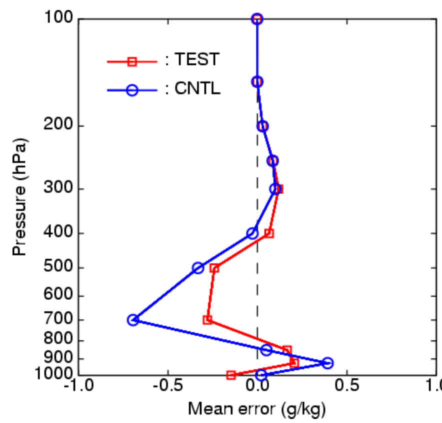

Fig. 1. ME of specific humidity in 48-hour forecasts against radiosonde observation over the tropics (20°N – 20°S) in August 2008 by TEST (red) and CNTL (blue).

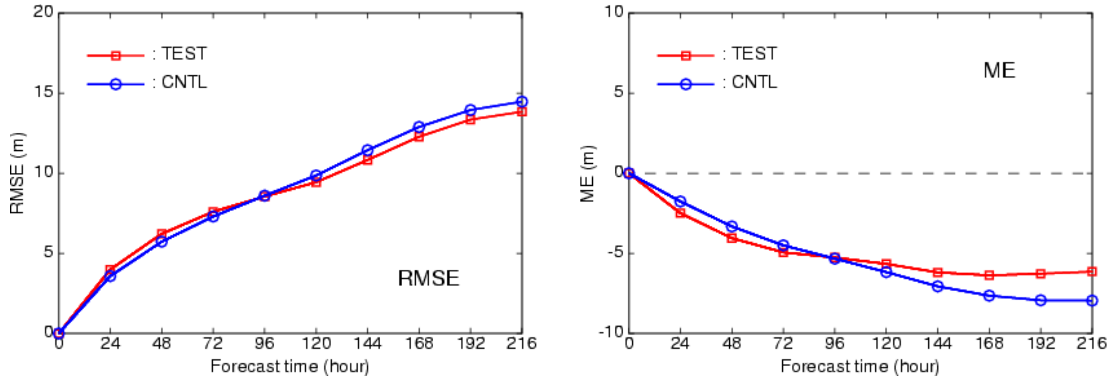

Fig. 2. RMSE (left) and ME (right) of 500 hPa geopotential height against the initial fields over the tropics in August 2008 by TEST (red) and CNTL (blue).

evaporation of detrained cloud water from the updraft in the cloud layer and increased evaporation of rain due to the modification of the parameterization scheme.

The root mean square errors (RMSE) and ME of 500 hPa geopotential height against the initial fields over the tropics are shown in Figure 2. The RMSE of TEST is larger in the early forecast hours and smaller in the later ones than that of CNTL. The ME shows a similar tendency except for its sign, which suggests a close relationship between the tendencies of RMSE and ME. It is likely that these tendencies of TEST in the early forecast hours are caused by the negative bias in temperature forecasts in the lower and middle troposphere, which is larger than that of CNTL (not shown). It is necessary to reduce these errors to enable implementation of the modification to the operational GSM.

References.

Arakawa, A. and W. H. Schubert, 1974: Interaction of a cumulus cloud ensemble with the large-scale environment, Part I. *J. Atmos. Sci.*, **31**, 674-701.

Cheng, M.-D. and A. Arakawa, 1997: Inclusion of Rainwater Budget and Convective Downdrafts in the Arakawa-Schubert Cumulus Parameterization. *J. Atmos. Sci.*, **54**, 1359-1378.

Kessler, E., 1969: On the distribution and continuity of water substance in atmospheric circulation. *Meteorological Monograph*, Vol. 10, No. 32, 84pp.

Kuo, H. L. and W. H. Raymond, 1980: A Quasi-One-Dimensional Cumulus Cloud Model and Parameterization of Cumulus Heating and Mixing Effects. *Mon. Wea. Rev.*, **108**, 991-1009.

Miyamoto, K. and T. Komori, 2008: Characteristics in the Moist Process of JMA-GSM. *The 88th American Meteorological Society Annual Meeting*, P3.15, 20-24 January 2008, New Orleans, USA.

Moorthi, S. and M. J. Suarez, 1992: Relaxed Arakawa-Schubert: A parameterization of moist convection for general circulation models. *Mon. Wea. Rev.*, **120**, 978-1002.

Pan, D.-M. and D. Randall, 1998: A cumulus parameterization with a prognostic closure. *Quart. J. Roy. Meteor. Soc.*, **124**, 949-981.

Randall, D. and D.-M. Pan, 1993: Implementation of the Arakawa-Schubert cumulus parameterization with a prognostic closure. *Meteorological Monograph/The representation of cumulus convection in numerical models.*, Vol. 24, No. 46, 137-144.

Inclusion of a Prognostic Equation for the Number Concentration of Cloud Ice in the Mesoscale Model

Masami Narita
Numerical Prediction Division, Japan Meteorological Agency
1-3-4 Otemachi, Chiyoda-ku, Tokyo 100-8122, Japan
E-mail: m_narita@naps.kishou.go.jp

The Japan Meteorological Agency operates a nonhydrostatic mesoscale model (MSM) with 5-km horizontal grid spacing (Saito et al., 2007). A bulk parameterization scheme for cloud microphysics based on Lin et al. (1983) and Murakami (1990) has been adopted in the MSM since the advent of the model's predecessor, developed at the Forecast Research Department of the Meteorological Research Institute (Ikawa and Saito, 1991). In this scheme, water classes are categorized into six forms: water vapor, cloud water, rain, cloud ice, snow and graupel. While mono-dispersion is assumed for the size distribution of cloud water and cloud ice, an exponential function is assumed for that of rain, snow and graupel.

Although the original cloud microphysics scheme predicted the mixing ratios of the six water classes and the number concentrations of cloud ice, snow and graupel, the microphysics of the operational MSM before December 2008 predicted only the mixing ratios in order to reduce the computational time taken. Furthermore, some simplification and elimination of the original cloud microphysics scheme were applied. These MSM modifications, especially the simplification of the conversion process of cloud ice to snow, made the growth of snow slow; as a result, excessive amounts of cloud ice remained in the atmosphere, as shown in Fig. 1 (a). When the number concentration of cloud ice (N_i) is not predicted, N_i is determined by the temperature or supersaturation ratio over ice for each step of time integration, and the diameter of cloud ice is determined only by the mixing ratio of cloud ice (q_i). Since an autoconversion concept is assumed in this scheme to parameterize the aggregation of cloud ice to form snow (Lin et al., 1983), the growth of cloud ice cannot be expressed and the conversion of cloud ice to snow becomes slow.

On the other hand, when N_i is predicted, it is independent of q_i, and the diameter of cloud ice is determined not only by q_i but also by N_i, and the growth of cloud ice and conversion of cloud ice to snow or graupel can be sophisticated (Murakami, 1990). Cloud microphysics using a

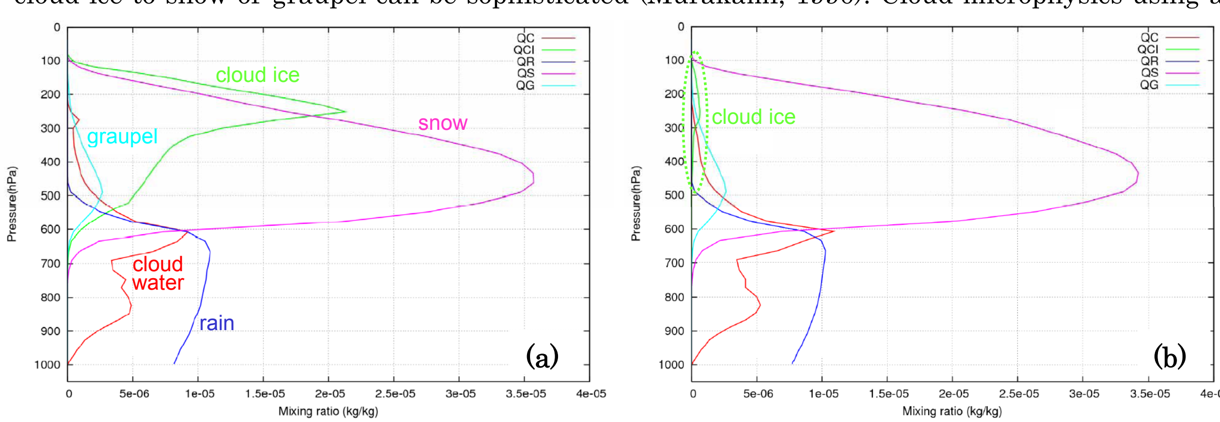

Fig. 1. Area-averaged vertical profiles of mixing ratios of cloud water, cloud ice, rain, snow and graupel [kg/kg] for 21 UTC on 22 August 2004 with MSM runs started at 15 UTC
(a) Number concentration of cloud ice not predicted
(b) Number concentration of cloud ice predicted.

prognostic equation for N_i eliminates excessive amounts of cloud ice, as shown in Fig. 1 (b). Furthermore, as shown in Fig. 2, the efficiency of conversion of cloud ice to snow becomes high, and the distribution of snowfall with the prognostic equation for N_i becomes better than that without prediction of N_i. Inclusion of the prognostic equation for N_i has been adopted in the operational MSM since December 2008.

References

Ikawa, M. and K. Saito, 1991: Description of a non-hydrostatic model developed at the Forecast Research Department of the MRI. *MRI Tech. Rep.* 28, 238 pp.

Lin, Y. -L., R. D. Farley and H. D. Orville, 1983: Bulk parameterization of the snow field in a cloud model. *J. Climate Appl. Meteor.*, **22**, 1065-1092.

Murakami, M., 1990: Numerical modeling of dynamical and microphysical evolution of an isolated convective cloud - the 19 July 1981 CCOPE cloud. J. *Meteor. Soc. Japan*, **68**, 107-128.

Saito, K., J. Ishida, K. Aranami, T. Hara, T. Segawa, M. Narita and Y. Honda, 2007: Nonhydrostatic atmospheric models and operational development at JMA. *J. Meteor. Soc. Japan*, **85B**, 271-304.

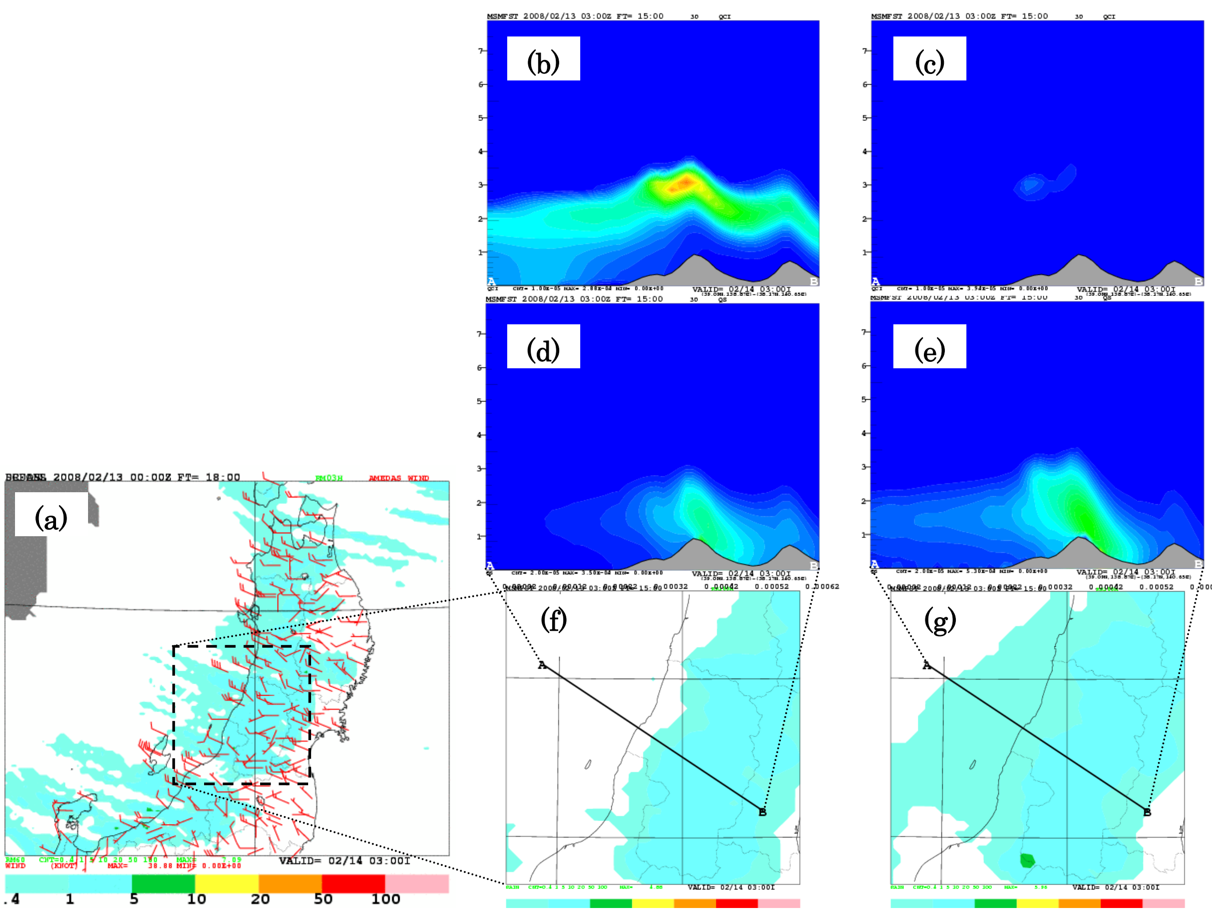

Fig. 2. Horizontal distributions of snowfall [mm/3 h] and vertical cross sections of mixing ratios of cloud ice and snow [kg/kg] at 18 UTC on 13 February 2008
(a) Observation of snowfall
(b), (d) and (f) Predicted vertical cross sections of mixing ratios of cloud ice and snow, and snowfall when the number concentration of cloud ice is not predicted
(c), (e) and (g) Equivalent to (b), (d) and (f), but for the case where the number concentration of cloud ice is predicted.

SPECIFICATION OF THE TURBULENT LENGTH SCALE l FOR THE COSMO MODEL BOUNDARY LAYER SCHEME

Veniamin Perov, Gdaly Rivin

Hydrometcenter of Russia, Moscow, Russia
perov@mecom.ru http://meteoinfo.ru

The original version of the scheme has been proposed by Bougeault and Lacarrere (Bougeault P., Lacarrere P., 1989).

They postulate that for each level in the atmosphere turbulent length scale l can be related to the distance that air parcel originating from this level, and having an initial kinetic energy equal to the mean turbulent kinetic energy (TKE) of the layer, can travel upward and downward before being stopped by buoyancy effects. If l_{up} and l_{down} are the bounds of integrals from temperature stratification (buoyancy) which equal to the mean TKE of the layer (given function), we can find these values taking the integrals.

The main advantage of Bougeault-Lacarrere method is to allow for remote effects of stable zones on the definition of l. For instance, using the integral with upper bound, the vertical depth of an unstable layer capped by a strong inversion is selected as the length scale for turbulence. Close to the surface, the low bound for the integral is zero and height above the surface is relevant length scale, then $L = \left(l_{up} \cdot l_{down}\right)^{1/2}$.

Finally following interpolation formula is employed: $1/l = 1/kz + 1/L$, (k is Karman constant). This method allows the length scale at any level to be affected not only by the stability at this level, but by the effect of remote stable zones ("non-local" l).

The algorithm of non-local calculation of l has been implemented in 1-D and 3-D COSMO-RU models.

The 3-D Mesoscale model COSMO-RU with the grid step of 14 km is adapted to the weather technological line of the Hydrometeorological centre of Russia and release of forecasts meteelements on 78 h on the European territory of Russia in an quasi-operative mode on the current initial data and conditions on borders is organized two times in day (00 and 12 hours UTC) on 1 node (2 processors Xeon 5345, 2.33GHz, with 4 cores each and 32 Gb operative memory on node, 64-bit, OS - RHEL5 (Red Hat Enterprise Linux 5), Intel C++ 10.0.26, Intel Fortran 10.0.26, Intel MPI 3.0). For these forecasts the HMC of Russia receives by *ftp* GME data from DWD and produces the forecasts for 78 h for the European part of Russia. Time of the run with 8 cores (1 x 8 - topology) is 3h 35 min (Rivin G., Rozinkina I., 2009).

The first runs show reasonable results for main meteorological fields in the atmospheric boundary layer. For instance, the fields of temperature and relative humidity at 1000 gPa after 78h forecast are shown in Figs. 1 and 2. The work will be continued and verifications for different meteorological situations will be done, as a comparison results with COSMO-RU current turbulent length scale (Blackadar formula).

Acknowledgements

The study was supported by the Russian Foundation for Basic Research (project no. 07-05-13566-ofi_ts).

References

Bougeault P., Lacarrere P. (1989). Parametrization of orography-induced turbulence in a mesobetascale model. MWR, **117,** p. 1872-1890.

Rivin G., Rozinkina I. (2009). The first steps of operational running of non-hydrostatic mesoscale model atmosphere COSMO-RU. Research Activities in Atmospheric and Oceanic Modelling, CAS/JSC WGNE, WMO (see this issue).

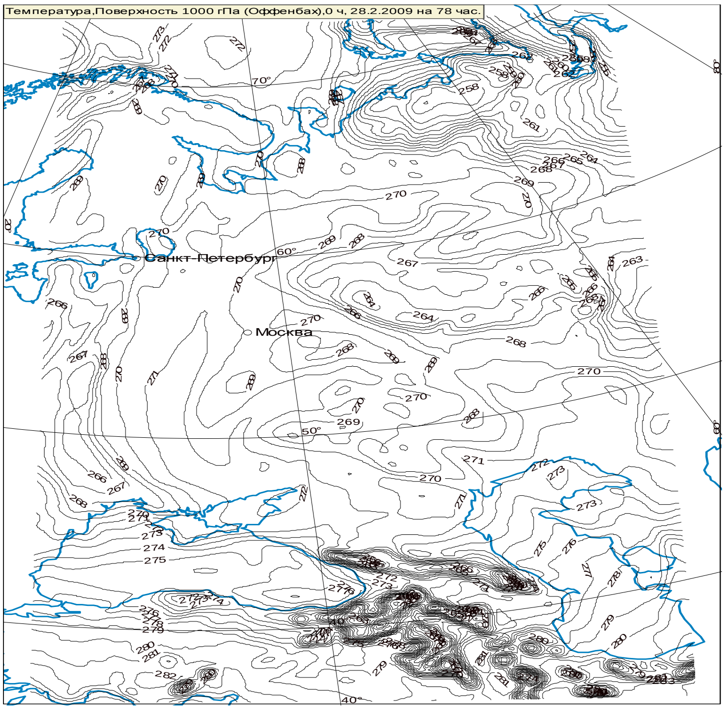

Fig. 1 Temperature at 1000 gPa after 78 hours forecast

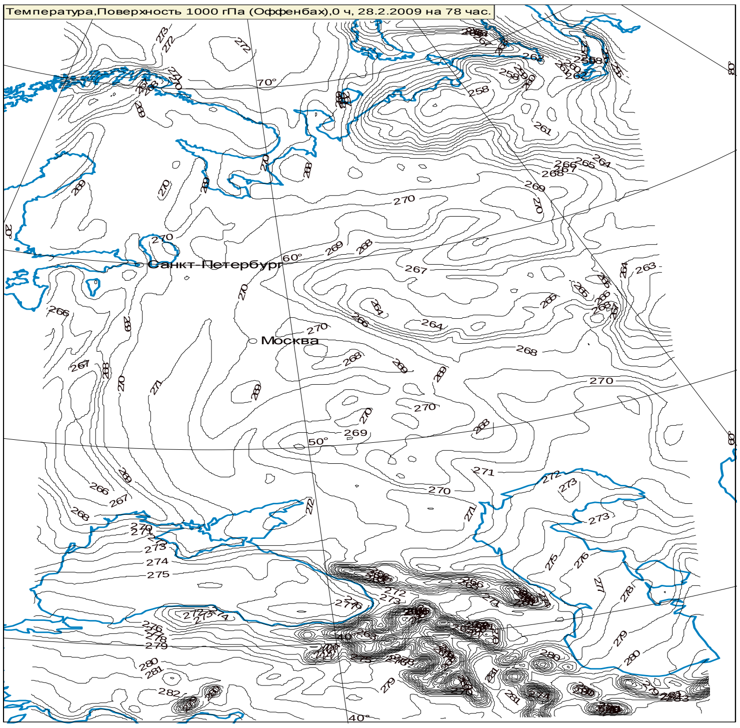

Fig. 2 Relative Humidity at 1000 gPa after 78 hours forecast

Numerical integration of two-equation turbulence closure scheme

V.Shnaydman

Department of Environmental Sciences,Rutgers University,USA

Email: volf@envsci.rutgers.edu

The developed atmospheric boundary layer modeling is based on two-equation turbulence closure, which included the turbulent kinetic energy (TKE) and dissipation equations along with Kolmogorov-Prandtl relationship. We recommended to include this more physical well-grounded approach in the prediction numerical operations as an alternative to Yamada-Mellor method and its modifications which. use TKE equation only with the set of empirical formulas.

Let's consider the non-stationary one-dimensional version of the turbulence closure when the advective terms play a secondary role in the turbulent exchange formation.

$$\frac{\partial E}{\partial t} = \eta - \mu + \alpha_E \frac{\partial}{\partial z} k \frac{\partial E}{\partial z} - \varepsilon , \frac{\partial \varepsilon}{\partial t} = \frac{\varepsilon}{E}\left\{a_1 \eta - a_2 \mu \right\}\Big] - a_4 \frac{\varepsilon^2}{E} + a_3 \frac{\partial}{\partial z} k \frac{\partial \varepsilon}{\partial z}$$

$$\eta = k\left[\left(\frac{\partial u}{\partial z}\right)^2 + \left(\frac{\partial v}{\partial z}\right)^2\right], \mu = \alpha_T \frac{g}{\theta_0} k \frac{\partial \theta}{\partial z}, \ k = \alpha_\varepsilon \frac{E^2}{\varepsilon}$$

The implicit time integration scheme is applied along with the successive sequence method. We consider the buoyancy and dissipation terms in the form which provide to fulfill the conditions of numerical stability and positive solution. TKE and dissipation equations are represented with the following expressions:

$$\frac{E_i^{m+1}(t+\delta t) - E_i(t)}{\delta t} = \eta_i^m + \alpha_E \left(\frac{\partial}{\partial z} k \frac{\partial E}{\partial z}^{m+1}\right)_i - \alpha_\varepsilon (2 E_i^{m+1} E_i^m - (E_i^m)^2) / k_i^m - \left(\frac{E_i^{m+1}}{E_i^m} \delta \mu_i^m + (1-\delta)\mu_i^m\right)$$

$$\frac{\varepsilon_i^{m+1}(t+\delta t) - \varepsilon_i(t)}{\delta t} = a_1 \frac{\varepsilon_i^m}{E_i^m} \eta_i^m + a_3 \left(\frac{\partial}{\partial z} k \frac{\partial \varepsilon_i^{m+1}}{\partial z}\right)_i - a_4 \frac{2\varepsilon_i^{m+1}\varepsilon_i^m - (\varepsilon_i^m)^2}{E_i^m} - \left(\frac{\varepsilon_i^{m+1}}{E_i^m} \delta \mu_i^m + \frac{\varepsilon_i^m}{E_i^m}(1-\delta)\mu_i^m\right)$$

$$\mu \geq 0, \delta = 1, \mu < 0, \delta = 0$$

We developed three approaches of numerical integration of two-equation turbulence closure to restore ABL vertical structure.

.1. The equations of the variables $E_i^{m+1}, \varepsilon_i^{m+1}$ in the instance $t + \delta t$ are presented in under mentioned expressions.

$$E_i^{m+1} = (D_i + d_{i+1} E_{i+1}^m + d_{i-1} E_{i-1}^m) / d_i , \ \varepsilon_i^{m+1} = (C_i + c_{i+1} \varepsilon_{i+1}^m + c_{i-1} \varepsilon_{i-1}^m) / c_i$$

2. We find the solution of equations () separately with the method of factorization.

$$d_{i+1} E_{i+1}^{m+1} - d_i E_i^{m+1} + d_{i-1} E_{i-1}^{m+1} = -D_i$$

$$d_{i+1} = \alpha_E \frac{k_{i+1}^m + k_i^m}{2(\delta z)^2}, d_{i-1} = \alpha_E \frac{k_i^m + k_{i-1}^m}{2(\delta z)^2}$$
$$d_i = 1/\delta t + d_{i+1} + d_{i-1} + \delta\mu_i^m / E_i^m + 2\alpha_\varepsilon E_i^m / k_i^m$$
$$D_i = E_i(t)/\delta t + \eta_i^m - (1-\delta)\mu_i^m + \alpha_\varepsilon (E_i^m)^2 / k_i^m$$

$$c_{i+1}\varepsilon_{i+1}^{m+1} - c_i \varepsilon_i^{m+1} + c_{i-1}\varepsilon_{i-1}^{m+1} = -C_i$$
$$c_{i+1} = a_3 \frac{k_{i+1}^m + k_i^m}{2(\delta z)^2}, c_{i-1} = a_3 \frac{k_i^m + k_{i-1}^m}{2(\delta z)^2}$$
$$c_i = 1/\delta t + c_{i+1} + c_{i-1} + a_2 \delta\mu_i^m / E_i^m + 2a_4 \varepsilon_i^m / E_i^m$$
$$C_i = \varepsilon_i(t)/\delta t + a_1 \frac{\varepsilon_i^m}{E_i^m}\eta_i^m - a_1 \frac{\varepsilon_i^m}{E_i^m}(1-\delta)\mu_i^m + \alpha_\varepsilon (\varepsilon_i^m)^2 / E_i^m$$

3. We solved the two-equation closure system with the matrix factorization method

$$d_{i+1} E_{i+1}^{m+1} - d_i E_i^{m+1} + d_{i-1} E_{i-1}^{m+1} - \varepsilon_i^{m+1} = -D_i$$
$$c_{i+1}\varepsilon_{i+1}^{m+1} - c_i \varepsilon_i^{m+1} + c_{i-1}\varepsilon_{i-1}^{m+1} - a_4 \frac{\alpha_\varepsilon}{k_i^m} E_i^{m+1} = -C_i$$
$$d_{i+1} = \frac{k_{i+1}^m + k_i^m}{2(\delta z)^2}, d_{i-1} = \frac{k_i^m + k_{i-1}^m}{2(\delta z)^2}$$
$$d_i = 1/\delta t + d_{i+1} + d_{i-1} + \delta\mu_i^m / E_i^m$$
$$D_i = E_i(t)/\delta t + \eta_i^m - (1-\delta)\mu_i^m$$
$$c_{i+1} = a_3 \frac{k_{i+1}^m + k_i^m}{2(\delta z)^2}, c_{i-1} = a_3 \frac{k_i^m + k_{i-1}^m}{2(\delta z)^2}$$
$$c_i = 1/\delta t + c_{i+1} + c_{i-1} + a_2 \delta\mu_i^m / E_i^m$$
$$C_i = \varepsilon_i(t)/\delta t + a_1 \frac{\varepsilon_i^m}{E_i^m}\eta_i^m - a_1 \frac{\varepsilon_i^m}{E_i^m}(1-\delta)\mu_i^m$$

The generalization of aforementioned approaches can be obtained if the advection terms are included in the TKE and dissipation equations.

Some assumptions about the application of developed approaches are suggested. The first approach can be used when the parameterization of ABL is applied in large scale prediction models where the horizontal step is much more than the ABL depth and is equal 50 km or more. The third approach can be applied when the horizontal step is comparable with the ABL depth which isn't more than 5 km. The second approach is acceptable for the intermediate horizontal scales. But it's the assumptions only and the solution of this problem is in question.